Submitted to ADVANCED MATERIALS

Supporting Information

DOI: 10.1002/adma.200902024

Conjugated Polymer/Metal Nanowire Heterostructure Plasmonic Antennas

Deirdre M. O'Carroll, Carrie E. Hofmann, Harry A. Atwater*

[*] Dr. Deirdre O'Carroll, Carrie E. Hofmann, Prof. Harry A. Atwater
Thomas J. Watson Sr. Laboratory of Applied Physics,
California Institute of Technology,
1200 East California Blvd., MC 128-95,
Pasadena, California 91125 (USA)
E-mail: doc@caltech.edu

Experimental Details

Nanostructural Characterization: Nanowire samples for scanning electron microscope analysis (field-emission scanning electron microscope, S-4100, Hitachi) were prepared by either depositing nanowires from suspension on gold-coated silicon substrates or by mounting a nanowire-filled alumina template onto a carbon pad, dissolving the alumina template using NaOH, rinsing gently with copious amounts of deionized water and drying under nitrogen gas flow. Transmission electron microscope (TEM) images, selected area diffraction patterns and energy dispersive X-ray spectra of individual gold and P3HT nanowires were acquired on a FEI Tecnai TF30UT transmission electron microscope **(**300 kV field-emission, equipped with a HAADF STEM detector, an Oxford energy dispersive x-ray detector, and a high resolution CCD camera). Nanowire samples were prepared for TEM analysis by depositing nanowires from suspension onto a holey carbon coated copper TEM grid (200 mesh, SPI Supplies) and allowing to dry. EDX peaks other than gold and sulfur were attributed to residual contamination from the TEM grid and chamber since they were also found in background EDX spectra (i.e., away from any nanowires). Bright-field and dark-field TEM analysis of multiple gold nanowires with lengths of a few microns (prepared under the same conditions as the gold-P3HT nanowires but with longer gold electrodeposition time) indicated that the electrodeposited gold nanowires were polycrystalline, with crystalline domains of up to 300 nm in size observed. Therefore, on the length scale of the gold nanowire segments employed in this work (i.e., < 250 nm) template-based electrodeposition can yield gold nanowire antennas with few or no crystallographic defects which is important for minimized damping of surface plasmon resonances.[16]

Gold-Polythiophene Nanowire Synthesis: Porous anodic alumina templates were purchased from Synkera Technologies, Inc. (13 mm diameter, 50 μm thick, 55 ± 6 nm nominal pore diameter, 5×10^9 cm^{-2} pore density, 12 % estimated porosity). Axial nanowire heterostructures were prepared by sequential electrodeposition in an ultrasonication bath. Firstly, a 400 nm thick layer of nickel was thermally evaporated onto the unbranched side of porous alumina templates. This nickel film served as a sacrificial working electrode to the pores of the alumina template. A ~ 13 mm diameter polypropylene film (1 mm thick) was coated with single-sided conductive copper tape and placed in a home-made cylindrical polyethylene holder and served as the back contact electrode of the electrochemical cell. The nickel coated side of an alumina template was placed in contact with the copper back electrode and an o-ring with an inner area of 0.11 cm^2 was coated with UV curable solvent-free epoxy and was placed on top of the alumina template. Subsequently a high density polyethylene tube (~13 mm in diameter) was pressed onto the o-ring to hold the alumina template in place and to act as a vessel for the electrolyte. UV optical adhesive was placed between the top of the polyethylene tube and o-ring to seal the cell and to ensure that only the pores were exposed to the electrolyte solution. The epoxy was cured by exposure to diffuse UV irradiation for 1 hour. Contact was made to the copper back electrode using a strip of copper tape and a 1 mm diameter steel wire counter electrode was placed within 3 mm of the nanoporous template surface. The resulting cell (Figure S1) was placed in a water bath in an ultrasonicator.

Sacrificial nickel nanowires were electrodeposited from nickel plating solution (Alfa Aesar) in the pores of the alumina template under constant applied current at –0.15 mA for 60 s (Keithley 286 source measure unit). Gold nanowires were electrodeposited from gold plating solution (Alfa Aesar) under pulsed applied current conditions at -0.3 mA for 15 pulses

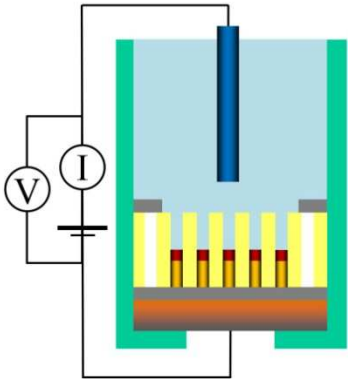

Figure S1. Schematic of the electrodeposition setup employed for the synthesis of axially heterostructured gold-P3HT nanowires.

(1 s duration, 50 % duty cycle, 0 mA bias; Keithley 286 source measure unit). Between each metal deposition step the plating solution was removed from the cell and the template was rinsed thoroughly with deionized water and various solvents and dried under nitrogen gas flow. For deposition of P3HT, 3-hexylthiophene (3HT) monomer (Sigma Aldrich) was electropolymerized at the tips of the gold nanowires under pulsed applied current conditions of +0.08 mA for 5 pulses (1 s duration, 50 % duty cycle, 0 mA bias) from a 20 g L^{-1} solution in boron trifluoride diethyl etherate ($BF_3{\cdot}O(C_2H_5)_2$) [13]. Subsequently, the alumina template, while remaining in the cell, was rinsed with $BF_3{\cdot}O(C_2H_5)_2$ followed by acetonitrile (× 3; to remove any residual 3HT monomer), acetone, methanol and IPA and dried under nitrogen gas flow. The polymerized P3HT remained at the tips of the gold nanowires as it was insoluble in $BF_3{\cdot}O(C_2H_5)_2$ and the other solvents used to rinse the template. Following the sequential electrodeposition / polymerization steps the gold-P3HT nanowires were released from the template by, firstly, etching the nickel working electrode and sacrificial nickel nanowires ($FeCl_3$ solution, 10 min), secondly, dissolving the alumina template (500 mL NaOH, 3 M, 1 h) and, subsequently, rinsing the nanowire residue with deionized water. Finally, the nanowires were dispersed in isopropyl alcohol by ultrasonication for between 10 and 30 s. From SEM analysis it was apparent that some gold wires (less than 20 %) did not appear to

have P3HT segments attached to the end, likely due to impurities or residual non-solvent within a fraction of the template pores prior to the deposition of the polymer. Neat P3HT nanowires were prepared under the same conditions as described above but without the gold nanowire electrodeposition step.

Optical Spectroscopy: P3HT thin films were spin coated at 6000 RPM from a 20 g L^{-1} solution of the polymer (electronic grade; American Dye Source, Inc.) in chloroform onto a solvent cleaned glass cover slip (film thickness ~125 nm, determined using spectroscopic ellipsometry and transmission measurements). The absorption spectrum of P3HT thin films and nanowires was acquired using an ellipsometer operating in transmission mode. The nanowires were embedded in optical epoxy and sandwiched between two quartz substrates to minimize light scattering. For all nanowire PL measurements, the nanowires were drop deposited on a glass cover slip from suspension, allowed to dry, and subsequently, embedded in flexible UV cured optical epoxy (refractive index, *n*, of 1.48; Norland Optical Adhesive 65, Norland Products, Inc.) with an additional glass cover slip placed on top. Single nanowire optical measurements were taken on an Axio Observer.Z1 Inverted Microscope (Carl Zeiss, Inc.) equipped with a digital color CCD camera (Infinity 2-3, Lumenera Corp.), a spectrometer consisting of an 150 mm-focal-length monochromator (slit width 450 μm, dual turret with 300 g mm^{-1} grating and alignment mirror; SpectraPro 2150i, Princeton Instruments/Acton Research Corp.) and liquid nitrogen cooled CCD camera (1340 × 100 pixels; Princeton Instruments Spec-10, Roper Scientific, Inc.). For single nanowire PL and PL lifetime measurements, either a 375 nm picosecond laser diode (1.5 mW, 70 - 300 ps pulse duration, 40 MHz; LDH-P-C-375B, PicoQuant GmbH) or a picosecond supercontinuum fiber laser (> 2 mW nm^{-1}, 455 - 1750 nm, 0.4 - 10 ps pulse duration, 40 MHz repetition rate; SC-400-4, Fianium Ltd.) was employed as the excitation source. For the latter excitation source, a beam sampler (400 - 700 nm, UV fused silica; BSF10-A1, Thorlabs, Inc.) was used to redirect

~ 5 % of the laser beam to a trigger diode assembly module (TDA 200, PicoQuant GmbH). An excitation spot area of about 1.6×10^{-6} cm^2 was typically employed. The SMA output of the trigger diode assembly module was attached to the input channel of a time-correlated single photon counting (TCSPC) module (PicoHarp 300, PicoQuant GmBH). A 425 - 475 nm band-pass filter was placed immediately after the beam sampler at of the output of the supercontinuum laser. For 375 nm excitation the laser diode driver supplied the trigger signal to the TCSPC module. The output of a single photon avalanche diode (SPAD) detector (50 μm active area, < 10 dark cps, < 50 ps timing resolution; PDM 50T, Micro Photon Devices) was used as the sensing input to the TCSPC module. The instrument response function (IRF) was measured to have a half width of 52 ps with the supercontinuum laser (i.e., limited by the response time of the SPAD) and ~ 80 ps with the 375 nm laser diode (limited by the minimum pulse duration of the laser diode). PL lifetime decays were acquired using PicoHarp software and analyzed using FluoFit software (PicoQuant GmbH). Individual nanowires were selected for PL lifetime analysis by placing a beam expander followed by a right angled mirror, a zero-aperture iris diaphragm (Edmund Optics, Inc.) to select individual nanowires and an achromatic lens before the SPAD detector which was mounted on an XYZ translation stage. The iris diaphragm was almost fully closed to reject stray light and detect PL from a single nanowire positioned within a region less than 5 μm in diameter on the sample at the SPAD. The entire system was aligned to the eyepiece cross hairs of the inverted microscope for accurate repositioning of nanowires in the collection path. For polarization-resolved excitation and collection a linear polarizer was placed after the beam expander in the collection path for surface-plasmon measurements or directly underneath the collection objective for PL measurements. A 100× oil immersion bright-field objective (numerical aperture of 1.3; Plan-Neofluar, Carl Zeiss, Inc.) was used for both surface-plasmon and PL spectroscopy. For surface plasmon spectroscopy the microscope was operated bright-field reflected light mode with full Köhler illumination for wide-field plane wave excitation the nanowire sample (a

variant of the Kretschmann–Raether configuration) [8]. A 10 mm fused silica prism (PS610, Thorlabs, Inc.) was placed on top of the sample to allow directly-transmitted (i.e., not scattered) lamp light to pass out of the sample while minimizing back reflection in to the objective at the top glass interface of the sample. Immersion oil (refractive index of 1.518; Immersol^{TM} 518F, Carl Zeiss, Inc.) was placed between the prism and the top glass substrate, between the microscope slide and the sample and between the oil immersion objective and the bottom glass cover slip of the sample. The PL was excited directly in transmission mode at 375 nm, while the scattered light spectra were excited through the high numerical aperture (NA) oil immersion collection objective (i.e., in reflection mode) under unpolarized broadband halogen lamp illumination. Not all wires exhibited clear exciton-plasmon coupling signatures in the PL spectra probably due to the distribution of gold nanowire lengths which would result in surface plasmon resonances that occur outside the wavelength range of P3HT light emission.

Theoretical Modelling: Normalized total decay rate was computed using 3D-FDTD software (Lumerical Solutions, Inc.) by integrating the Poynting vector over a closed surface containing only a dipole emitter which was embedded in an environment whose wavelength-dependent dielectric constant corresponded to that of P3HT (extracted from Ref. [20]) which was placed near the end of a gold nanowire. Both the gold and P3HT containing the dipole emitter were embedded in a homogeneous environment with refractive index of 1.48. The radiative decay rate (normalized to that of dipole emitter without presence of P3HT or gold) was computed by integrating the Poynting vector over a closed surface incorporating the dipole emitter in P3HT and the gold nanowire thereby including non-radiative losses to the metal.[18] The non-radiative and radiative decay rate enhancements were calculated by normalizing to those of a dipole emitter in P3HT without proximity to a gold nanowire (Figure S2).

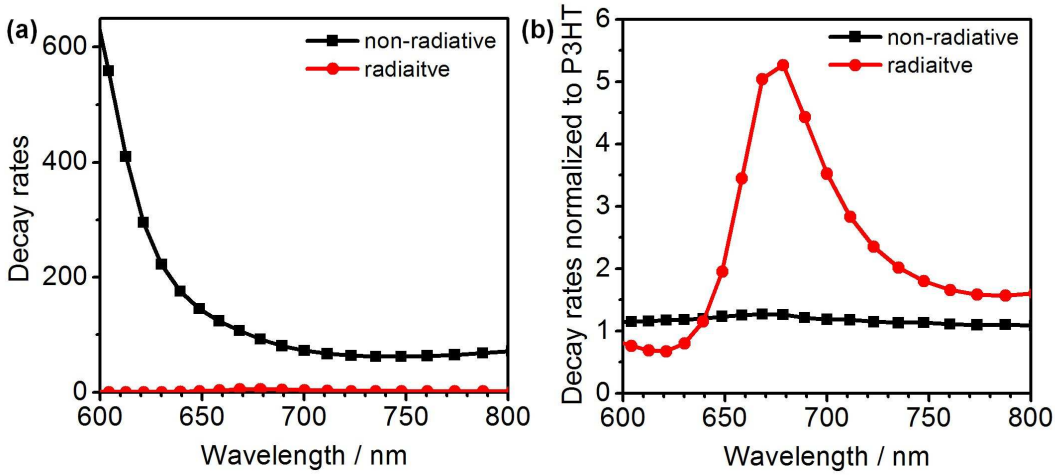

Figure S2. Non-radiative and radiative decay rates of a dipole emitter in P3HT placed 10 nm from the end of a gold nanowire (60 nm diameter, 190 nm length). A background refractive index of 1.48 was employed. (a) Decay rates calculated directly from the integrated Poynting vector. (b) Decay rate enhancements calculated by normalizing the decay rates in (a) to the decay rates of a dipole emitter in P3HT in the absence of the gold nanowire. This yields information on changes in the decay rates that occur due solely due to the presence of the gold nanowire antenna.

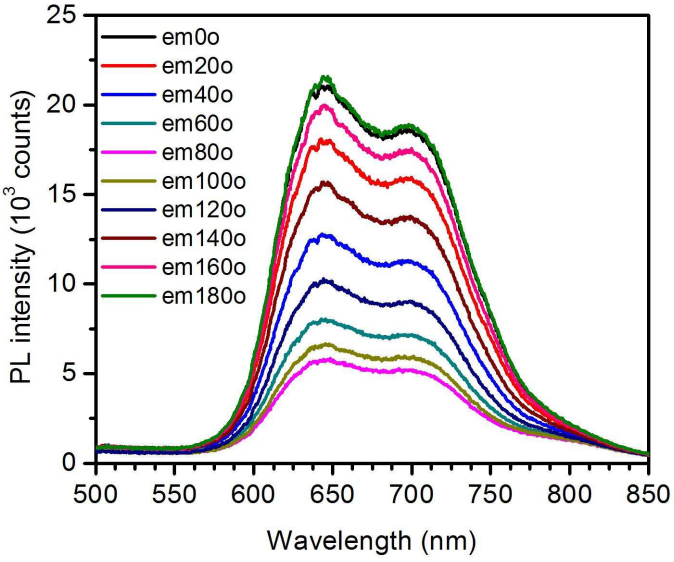

Figure S3. Polar plot of PL intensity from a single gold-P3HT nanowire as a function of collection polarization angle (red) and excitation laser polarization angle (blue).

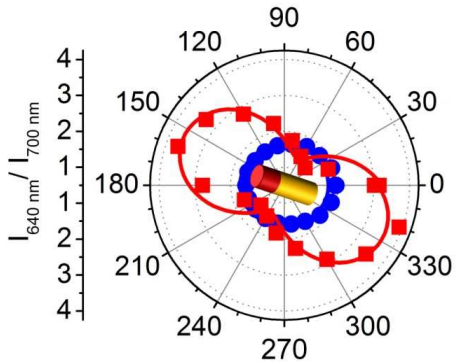

Figure S4. Polar plot of PL intensity from a single gold-P3HT nanowire as a function of collection polarization angle (red) and excitation laser polarization angle (blue).

Theoretical polar plots of field intensity in the P3HT segment and at the surface of the gold nanowire versus excitation polarization angle are shown in Figure S5a and Figure S5b. The nanowire was oriented vertically (i.e., with long axis at 90^o) in the simulations. At 538 nm, the plot shows a dipole-like profile with lobes oriented almost transversely (i.e., at 30^o and 210^o within the P3HT segment and at 15^o and 195^o at the gold nanowire surface) to the nanowire long axis, consistent with excitation of the transverse surface plasmon resonance of the gold nanowire. The polar plot was not perfectly oriented transversely to the wire long axis, most likely due to either the off-normal plane wave incidence angle (10^o) employed in the simulations which may have excited longitudinal and transverse field components or the existence of a multipole surface plasmon mode (e.g., 3λ/2 mode) in the wavelength range of the transverse surface plasmon resonance. At 673 nm, the polar plot also showed a dipole-like profile with lobes oriented along the nanowire long axis (i.e., at 90^o and 270^o) as expected for a longitudinal surface plasmon resonance of the gold nanowire.

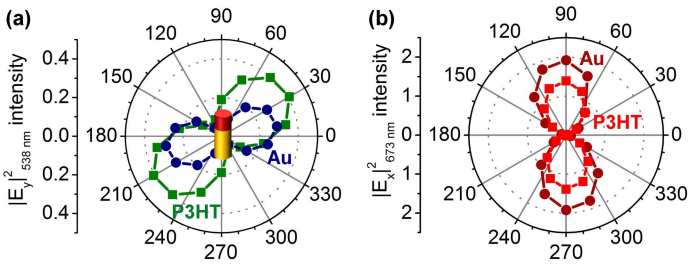

Figure S5. (a) Theoretical plot of near-field intensity monitored at a point 5 nm from a gold nanowire surface (190 nm long, 60 nm in diameter; circles) and within a P3HT segment at a point 10 nm from the end of a gold nanowire (squares) versus excitation polarization angle at 538 nm and (b) at 673 nm (from 3-dimensional FDTD simulations). Plane wave excitation with an incidence angle of 10^o off normal to break symmetry was employed.